CENTRAL RESEARCH LIBRARY
DOCUMENT COLLECTION

OAK RIDGE NATIONAL LABORATORY
operated by
UNION CARBIDE CORPORATION
NUCLEAR DIVISION
for the
U.S. ATOMIC ENERGY COMMISSION

OAK RIDGE NATIONAL LABORATORY
CENTRAL RESEARCH LIBRARY
DOCUMENT COLLECTION
LIBRARY LOAN COPY
DO NOT TRANSFER TO ANOTHER PERSON
If you wish someone else to see this document, send in name with document and the library will arrange a loan.
UCN-7969
13 3-67)

LOCKHEED MARTIN ENERGY RESEARCH LIBRARIES
3 4456 0513858 9

ORNL-TM-3517
COPY NO. - 46
DATE - March 22, 1972

Neutron Physics Division

NEUTRON AND GAMMA-RAY FLUENCE TRANSMITTED THROUGH A SLAB OF BORATED POLYETHYLENE - A MILESTONE CALCULATION

C. E. Burgart*

Abstract

A multigroup Monte Carlo code, a two-dimensional discrete ordinates code, and a one-dimensional discrete ordinates code were utilized in a milestone radiation transport calculation. The neutron energy spectrum and the neutron and gamma-ray fluence at points located a large distance from a slab of borated polyethylene were calculated. A line beam of neutrons with a ^{235}U fission spectrum is assumed normally incident on the slab. Identical multigroup cross sections were employed, thus providing a rigorous comparison of the transport methods alone. A pseudo-energy point cross-section Monte Carlo code was also utilized. This provided a check on the cross-section processing codes. The methods yield nearly identical results for points located within 30° of a normal to the slab. The agreement becomes less satisfactory at greater angles. However, possible explanations for the observed discrepancies are given.

NOTE:
This Work Supported By
DEFENSE NUCLEAR AGENCY
Under Subtask PE07401

*Present address: Science Applications, Inc., Albuquerque, New Mexico 87108

This report was prepared as an account of work sponsored by the United States Government. Neither the United States nor the United States Atomic Energy Commission, nor any of their employees, nor any of their contractors, subcontractors, or their employees, makes any warranty, express or implied, or assumes any legal liability or responsibility for the accuracy, completeness or usefulness of any information, apparatus, product or process disclosed, or represents that its use would not infringe privately owned rights.

The MORSE multigroup Monte Carlo code,[1] the DOT two-dimensional discrete ordinates code[2] with SPACETRAN void transport code,[3] and the ANISN one-dimensional discrete ordinates code[4] were utilized in a milestone radiation transport calculation. Identical multigroup cross sections were used by all three codes. Thus, a comparison between the results of calculations using these codes provides a basis for comparison of transport techniques and data handling rather than verification of the cross sections. Many aspects of these codes have been investigated in the past. However, this comparison of the three codes has been quite constructive and provides an added check point. Several important aspects of these codes were checked through these calculations. Specifically, the DOT-SPACETRAN coupling, MORSE secondary gamma-ray generation, and the MORSE next-flight estimation subroutines have been verified by these calculations. In addition to these multigroup codes, the pseudo-energy point cross-section Monte Carlo codes 06R (neutron transport) and OGRE (gamma-ray transport) were utilized.[5,6] This provides a check on the cross-section processing codes in addition to 06R and OGRE.

The neutron energy spectrum and neutron and gamma-ray total fluence are desired at several hypothetical point detectors located at large distances from a borated polyethylene slab. The configuration of interest is shown in Fig. 1. A monodirectional neutron beam with a ^{235}U fission source energy spectrum is normally incident at a point on the polyethylene. Two thicknesses of 2% borated polyethylene are of interest - 2.54 and 15.24 cm. The composition is given in Table 1. All detectors are located 100 meters from the intersection of the uncollided neutron beam and the face of the slab toward the detectors. The four angles of interest (θ))

LOCKHEED MARTIN ENERGY RESEARCH LIBRARIES

3 4456 0513858 9

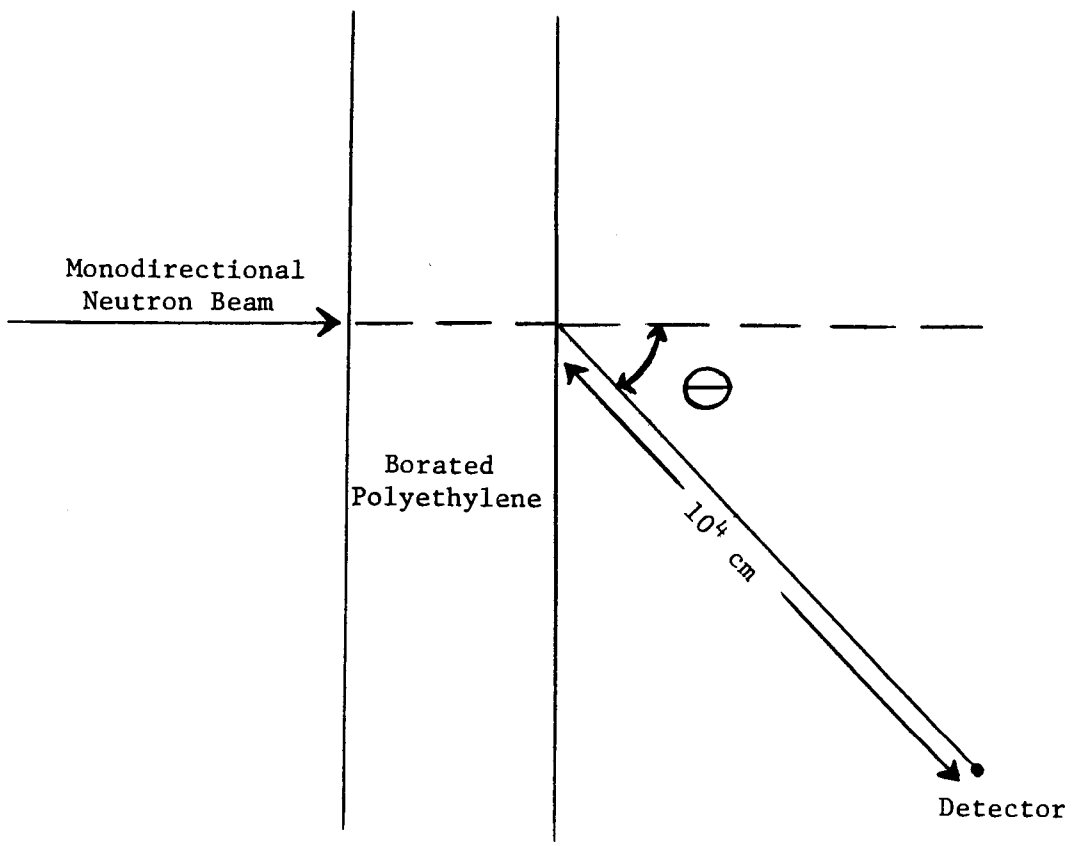

Fig. 1. Configuration of Interest

Table 1. Borated Polyethylene Composition

Element	Atomic Concentration (atoms/barn.cm)
^{12}C	0.037873
H	0.075746
^{10}B	0.0010019

and their cosines (μ) are given in Table 2. The assumption is made that the detector point is located far enough away from the slab such that all particles emerging from the slab view the detector at a distance R and at an angle θ with respect to a normal. With this assumption, the problem is one dimensional and may be solved by the discrete ordinates code ANISN; three multidimensional techniques were also used. These were the two-dimensional discrete ordinates code DOT, together with the void transport code SPACETRAN, the multigroup Monte Carlo code MORSE with the SAMBO analysis package,[7] and 06R pseudo-point cross-section Monte Carlo neutron transport code coupled with OGRE gamma-ray transport code. Three of these codes - ANISN, DOT, and MORSE - utilized the identical multigroup cross sections. Thus, this comparison does not check the multigroup cross-section preparation or the basic cross-section data, but it does provide an exact basis for comparison of the transport methods. The Monte Carlo codes 06R and OGRE utilize entirely independent cross-section processing codes. Results from these codes, compared with the previous calculations, provide a check on both the multigroup processing codes and pseudo-point cross-section processing codes, and also the pseudo-point cross-section Monte Carlo codes.

The neutron and gamma-ray cross sections for ^{12}C, H, and ^{10}B were from ENDF/B-II data. The neutron multigroup cross sections were generated utilizing the SUPERTOG code.[8] The 104-fine-group neutron cross sections were reduced to 22 groups using ANISN with fission spectrum source. The gamma-ray multigroup cross sections were generated using MUG.[9] The neutron-gamma-ray coupling utilized yield data from the POPOP4 library[10] (data sets 010101, 060101, 060301, and 05100201). The neutron-gamma-ray coupled

Table 2. Detector Numbers, Angles, and Cosines

Detector Number	1	2	3	4
Angles (θ)	9.7°	26.3°	42.9°	81.7°
Cosines (μ)	0.98561	0.89632	0.73218	0.14447

multigroup cross-section set was generated using the SAMPLE COUPLING CODE (ASCC).[11] The multigroup cross sections are in a 22-18 group structure with P_3 coefficients.* The energy group structure and source energy spectrum are given in Table 3. The source has been normalized to 1 incident neutron. The pseudo-point cross sections for 06R were generated using NUSECT.[5] The neutron-gamma-ray coupling matrix utilized by 06R was identical to that used in preparing the coupled multigroup cross sections.

The ANISN cases utilized an S_{32} quadrature. (The S_{32} quadrature set is given in Table 4.) The 2.54- and 15.24-cm-thick slabs had 12 and 62 spatial mesh points, respectively. The last two mesh points near the surface of the slab on the side toward the detector were 0.12 cm apart. Thus, the extrapolation across the mesh points near the surface would cause little error. The location of the detectors of interest were selected so that four of the angles in the S_{32} discrete angle quadrature set would intersect the detectors. The boundary angular fluences given by ANISN as particles/unit weight, were multiplied by their respective cosines and divided by $4\pi R^2$ to obtain the particle fluences at the detector points in terms of particles/cm^2.

The DOT-SPACETRAN calculations were run in cylindrical geometry with an asymmetric 100-angle quadrature set. (The S-100 quadrature set is given in Table 4.) The beam source was incident on the centerline of the cylinder, and the leakage fluence out the other end was utilized as the source for the SPACETRAN calculation. For the 15.24-cm case, 32 axial mesh points, and 25 radial mesh points out to 50-cm radius were utilized. Two different mesh spacings were used in the 2.54-cm case; 12 axial and 25 radial, and 12 axial and 50 radial intervals. The outer radius was assumed to be 50 cm in both cases.

*These multigroup cross sections are available from the Radiation Shielding Information Center.

Table 3. Group Structures and Source Spectrum

Neutron Group Number	Upper Energy (eV)	Fraction of Source Neutrons in Group	Gamma Group Number	Upper Energy (MeV)
1	15.0+6*	1.566-4	1	10.0
2	12.2+6	8.979-4	2	8.0
3	10.0+6	3.496-3	3	6.5
4	8.18+6	1.397-2	4	5.0
5	6.36+6	3.473-2	5	4.0
6	4.96+6	3.522-2	6	3.0
7	4.06+6	1.078-1	7	2.5
8	3.01+6	8.941-2	8	2.0
9	2.46+6	2.330-2	9	1.66
10	2.35+6	1.209-1	10	1.33
11	1.83+6	2.191-1	11	1.0
12	1.11+6	1.994-1	12	0.8
13	5.50+5	1.360-1	13	0.6
14	1.11+5	1.557-2	14	0.4
15	3.35+3	0	15	0.3
16	5.83+2	0	16	0.2
17	1.01+2	0	17	0.1
18	2.90+1	0	18	0.05
19	1.07+1	0		0.01
20	3.06+0	0		
21	1.12+0	0		
22	0.414+0	0		
	0.025+0			

*Read as 15.0×10^6 eV.

Table 4. Quadrature Sets

	DOT S-100			ANISN S-32	
Angle	Weight	Eta	Mu	Mu	Weight
1	0.0	-0.99967998	-0.25297999-1	-1.00000	0
2	0.19632999-3*	-0.99967998	-0.16594999-1	-9.97260-1	3.50930-3
3	0.19632999-3	-0.99967998	0.16594999-1	-9.85610-1	8.13720-3
4	0.0	-0.99835998	-0.57247996-1	-9.54760-1	1.26960-2
5	0.45976997-3	-0.99835998	-0.37554000-1	-9.34910-1	1.71370-2
6	0.45976997-3	-0.99835998	0.37554000-1	-8.96320-1	2.14180-2
7	0.0	-0.99597996	-0.89575946-1	-8.49370-1	2.65990-2
8	0.72320993-3	-0.99597996	-0.58759999-1	-7.94480-1	2.93420-2
9	0.72320993-3	-0.99597996	0.58759999-1	-7.32180-1	3.29110-2
10	0.0	-0.99253994	-0.12191999	-6.63040-1	3.61730-2
11	0.98416000-3	-0.99253994	-0.79976976-1	-5.87720-1	3.90970-2
12	0.98416000-3	-0.99253994	0.79976976-1	-5.06900-1	4.16560-2
13	0.0	-0.98804998	-0.15412998	-4.21350-1	4.38260-2
14	0.12450998-2	-0.98804998	-0.10110998	-3.81870-1	4.55870-2
15	0.12450998-2	-0.98804998	0.10110998	-2.89290-1	4.69220-2
16	0.0	-0.98250997	-0.18620998	-1.44470-1	4.78190-2
17	0.15035998-2	-0.98250997	-0.12214994	-4.83080-2	4.82700-2
18	0.15035998-2	-0.98250997	0.12214994	4.83080-2	4.82700-2
19	0.0	-0.97592998	-0.21807998	-1.44470-1	4.78190-2
20	0.17619999-2	-0.97592998	-0.14305997	2.39290-1	4.69220-2
21	0.17619999-2	-0.97592998	0.14305997	3.31870-1	4.55870-2
22	0.0	-0.96831995	-0.24970996	4.21350-1	4.38260-2
23	0.20180000-2	-0.96831995	-0.16380996	5.06900-1	4.16560-2
24	0.20180000-2	-0.96831995	0.16380996	5.87720-1	3.90970-2
25	0.0	-0.95967996	-0.28109998	6.63040-1	3.61730-2

*Read as $0.19632999 \times 10^{-3}$.

Table 4 (continued)

DOT S-100				ANISN S-32	
Angle	Weight	Eta	Mu	Mu	Weight
26	0.22715000-2	-0.95967996	-0.18438995	-7.82180-1	3.29110-2
27	0.22715000-2	-0.95967996	0.18438995	7.94480-1	2.93420-2
28	0.0	-0.95002997	-0.31215996	8.49370-1	2.54990-2
29	0.25249999-2	-0.95002997	-0.20476997	-8.96320-1	2.14180-2
30	0.25249999-2	-0.95002997	0.20476997	9.34910-1	1.71370-2
		-0.95002997			
31	0.0	-0.93936998	-0.34290999	9.64760-1	1.26960-2
32	0.27734998-2	-0.93936998	-0.22493994	-9.85610-1	8.13720-3
33	0.27734998-2	-0.93936998	0.22493994	9.97260-1	3.50930-3
34	0.0	-0.86505997	-0.50166994		
35	0.24296999-1	-0.86505997	-0.43339998		
36	0.12844998-1	-0.86505997	-0.14887995		
37	0.12844998-1	-0.86505997	0.14887996		
38	0.24296999-1	-0.86505997	0.43339998		
39	0.0	-0.67939997	-0.73376995		
40	0.26850998-1	-0.67939997	-0.67941999		
41	0.84993988-2	-0.67939997	-0.43339998		
42	0.19095998-1	-0.67939997	-0.14887995		
43	0.19095998-1	-0.67939997	0.14887995		
44	0.84993988-2	-0.67939997	0.43339998		
45	0.26850998-1	-0.67939997	0.67941999		
46	0.0	-0.43338996	-0.90120995		
47	0.24296999-1	-0.43338996	-0.86506999		
48	0.84993988-2	-0.43338996	-0.67940998		
49	0.27305000-1	-0.43338996	-0.43339998		
50	0.68163984-2	-0.43338996	-0.14886999		

Table 4 (continued)

DOT S-100				ANISN S-32
Angle	Weight	Eta	Mu	
51	0.68163984-2	-0.43338996	0.14886999	
52	0.27305000-1	-0.43338996	0.43339998	
53	0.84993988-2	-0.43338996	0.67940998	
54	0.24296999-1	-0.43338996	0.86506999	
55	0.0	-0.22777998	-0.97370994	
56	0.83636977-2	-0.22777998	-0.95898998	
57	0.64835995-2	-0.22777998	-0.85181999	
58	0.96394978-2	-0.22777998	-0.66899997	
59	0.34407999-2	-0.22777998	-0.42675996	
60	0.91448985-2	-0.22777998	-0.14658999	
61	0.91448985-2	-0.22777998	0.14658999	
62	0.34407999-2	-0.22777998	0.42675996	
63	0.96394978-2	-0.22777998	0.66899997	
64	0.64835995-2	-0.22777998	0.85181999	
65	0.83636977-2	-0.22777998	0.95898998	
66	0.0	-0.76249957-1	-0.99708998	
67	0.85643977-2	-0.76249957-1	-0.98200995	
68	0.66391975-2	-0.76249957-1	-0.87226999	
69	0.98707974-2	-0.76249957-1	-0.68506998	
70	0.35233998-2	-0.76249957-1	-0.43699998	
71	0.93643963-2	-0.76249957-1	-0.15010995	
72	0.93643963-2	-0.76249957-1	0.15010995	
73	0.35233998-2	-0.76249957-1	0.43699998	
74	0.98707974-2	-0.76249957-1	0.68506998	
75	0.66391975-2	-0.76249957-1	0.87226999	

Table 4 (continued)

DOT S-100				ANISN S-32
Angle	Weight	Eta	Mu	
76	0.85643977-2	-0.76249957-1	0.98200995	
77	0.0	0.96028990	-0.27900428	
78	0.25307138-1	0.96028990	-0.18343455	
79	0.25307138-1	0.96028990	0.18343455	
80	0.0	0.79666644	-0.60441917	
81	0.35623208-1	0.79666644	-0.52553236	
82	0.19972049-1	0.79666644	-0.18343455	
83	0.19972049-1	0.79666644	0.18343455	
84	0.35623208-1	0.79666644	0.52553236	
85	0.0	0.52553236	-0.85077357	
86	0.35623208-1	0.52553236	-0.79666644	
87	0.16251847-1	0.52553236	-0.52553236	
88	0.26551608-1	0.52553236	-0.18343455	
89	0.26551608-1	0.52553236	0.18343455	
90	0.16251847-1	0.52553236	0.52553236	
91	0.35623208-1	0.52553236	0.79666644	
92	0.0	0.18343455	-0.98303187	
93	0.25307138-1	0.18343455	-0.96028990	
94	0.19972049-1	0.18343455	-0.79666644	
95	0.26551608-1	0.18343455	-0.52553236	
96	0.18840149-1	0.18343455	-0.18343455	
97	0.18840149-1	0.18343455	0.18343455	
98	0.26551608-1	0.18343455	0.52553236	
99	0.19972049-1	0.18343455	0.79666644	
100	0.25307138-1	0.18343455	0.96028990	

The MORSE-SAMBO calculations utilized next-flight estimation to calculate the quantities of interest. Two slightly different estimators were utilized; one estimates to a selected outgoing group (referred to as estimator S), and the other estimates to all lower energy groups (referred (referred to as estimator A). Importance sampling in the form of non-leakage was utilized. The 06R and OGRE Monte Carlo calculations also utilized next-flight estimation. Leakage was permitted. The version of OGRE utilized in these calculations treated pair production as absorption.

As an integral check on the transport, the total fluence integrated over the volume of the 15.24-cm-thick slab calculated by the three multi-group codes is compared in Table 5. The total fluence is given as neutron·cm/eV. The MORSE results were obtained using a collision density estimator and statistics were not calculated. Due to the few number of collisions occurring above 2.35 MeV, meaningful estimates were not obtained on the MORSE results above this energy. The results labeled "Uncollided Total Path Length" were obtained analytically. This comparison checks in an integral sense the source description and transport in the slab.

Table 6 contains some of the detailed results for the 15.24-cm case. Given for each detector and each method is the total neutron fluence and total gamma-ray fluence. The results labeled "MORSE(A)" utilized estimator A. Those labeled "MORSE(S)" utilized estimator S. The estimated fractional standard deviations are indicated in parentheses. Figure 2 shows the neutron energy spectrum for the 15.24-cm case for detector 2 (26.3°) for each multigroup method. Error bars equal to one standard deviation are plotted when the fractional standard deviation exceeds 10%. Similar results for the 2.54-cm case are given in Table 7. The only exception is the

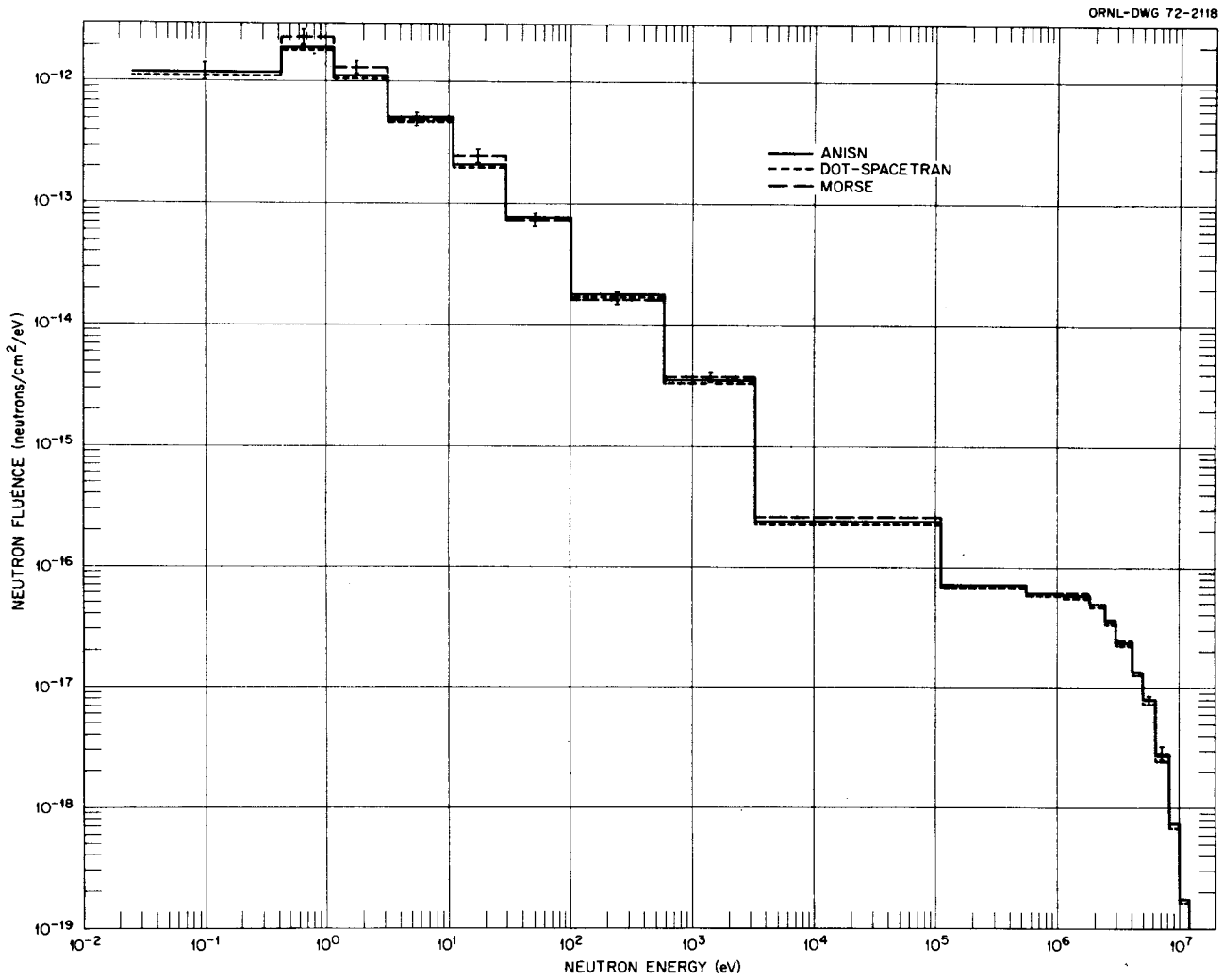

Neutron Energy Spectrum for 15.24 cm Slab, Detector 2.

Figure 2

Table 5. Total Neutron Fluence in 15.24-cm-thick Slab

Group	Total Fluence (neutron.cm/eV) ANISN	DOT	MORSE	Uncollided Total Path Length
1	4.82-10*	4.81-10	-	4.16-10
2	3.42-9	3.42-9	-	2.89-9
3	1.55-8	1.55-8	-	1.32-8
4	5.88-8	5.86-8	-	4.82-8
5	1.79-7	1.80-7	-	1.41-7
6	2.84-7	2.84-7	-	1.85-7
7	6.45-7	6.44-7	-	4.16-7
8	1.07-6	1.07-6	-	6.25-7
9	1.41-6	1.41-6	-	8.07-7
10	1.55-6	1.55-6	1.57-6	8.12-7
11	2.14-6	2.13-6	2.15-6	8.74-7
12	2.94-6	2.93-6	2.94-6	7.46-7
13	4.73-6	4.68-6	4.69-6	3.90-7
14	1.93-5	1.91-5	1.97-5	9.75-8
15	3.03-4	2.98-4	3.09-4	-
16	1.60-3	1.57-3	1.59-3	-
17	6.86-3	6.74-3	6.77-3	-
18	1.91-2	1.87-2	1.91-2	-
19	4.70-2	4.61-2	4.82-2	-
20	1.09-1	1.07-1	1.10-1	-
21	1.97-1	1.93-1	1.94-1	-
22	2.03-1	1.99-1	2.00-1	-

*Read as 4.82×10^{-10} eV.

Table 6. Particle Fluence for the 15.24-cm Slab

Detector Number	1	2	3	4
COSINE	0.98561	0.89632	0.73218	0.14447
ANGLE	9.7°	26.3°	42.9°	81.7°
	Neutron Fluence (neutrons/cm^2)			
ANISN	3.57-10	2.74-10	1.86-10	1.20-11
DOT-SPACETRAN	3.54-10	2.58-10	1.37-10	0.97-11
MORSE(A)	3.72-10(.04)	2.85-10(.05)	1.69-10(.06)	1.08-11(.16)
MORSE(S)	3.60-10(.03)	2.72-10(.03)	1.59-10(.04)	1.06-11(.11)
06R	3.60-10(.04)	2.69-10(.05)	1.55-10(.07)	0.91-11(.21)
	Gamma-Ray Fluence (photons/cm^2)			
ANISN	8.86-10	8.31-10	7.06-10	9.29-11
DOT-SPACETRAN	8.49-10	7.94-10	6.41-10	6.93-11
MORSE(A)	8.45-10(.04)	7.93-10(.04)	6.75-10(.04)	9.27-11(.06)
MORSE(S)	8.87-10(.03)	8.30-10(.03)	7.08-10(.03)	9.66-11(.05)
06R-OGRE	9.31-10(.04)	8.69-10(.04)	7.34-10(.04)	9.72-11(.10)

Table 7. Particle Fluence for the 2.54-cm Slab

Detector Number	1	2	3	4
COSINE	0.98561	0.89632	0.73218	0.14447
ANGLE	9.7°	26.3°	42.9°	81.7°
	Neutron Fluence (neutrons/cm^2)			
ANISN	1.62-9	1.37-9	9.54-10	8.59-11
DOT-SPACETRAN	1.62-9	1.33-9	8.67-10	7.44-11
DOT-SPACETRAN(2)	1.62-9	1.31-9	8.38-10	7.20-11
MORSE(A)	1.61-9(.01)	1.35-9(.01)	9.40-10(.01)	7.69-11(.03)
MORSE(S)	1.65-9(.01)	1.37-9(.01)	9.40-10(.01)	8.99-11(.03)
06R	1.59-9(.01)	1.36-9(.01)	9.68-10(.01)	8.00-11(.03)
	Gamma-Ray Fluence (photons/cm^2)			
ANISN	7.15-11	7.13-11	7.13-11	4.22-11
DOT-SPACETRAN	6.99-11	7.15-11	7.33-11	4.51-11
DOT-SPACETRAN(2)	7.03-11	7.18-11	7.32-11	4.48-11
MORSE(A)	6.77-11(.05)	6.80-11(.05)	6.76-11(.05)	3.96-11(.05)
MORSE(S)	6.86-11(.05)	6.87-11(.05)	6.74-11(.05)	3.94-11(.05)
06R-OGRE	6.98-11(.04)	6.96-11(.04)	6.85-11(.04)	3.98-11(.05)

addition of the results labeled "DOT-SPACETRAN(2)." The results shown in this line are those with 50 radial mesh points. The neutron energy spectrum for detector 4 (81.7°) for the 2.54-cm case is shown in Fig. 3.

Two observations should be made concerning Table 7 at this time. First, the DOT-SPACETRAN (2) calculations were performed to investigate the accuracy of the extrapolation across mesh points. This effect would be most significant at the more oblique angles. The addition of mesh points decreased the fluence at the detectors by less than 4%. Second, the MORSE results for the total neutron fluence at 81.7° differ from one another more than the estimated statistics indicate they should. This discrepancy is attributed to the next-flight estimator A. Both estimators utilize next-flight estimation at each real collision to obtain estimates of the flux at the point detectors. This estimation utilizes an array containing products including the probability of scatter from the incoming group to each possible outgoing group and the value of the angular distribution for each outgoing group at the angle between the incoming neutron direction and direction from the collision site to the point detector. Since the angular distributions associated with some group-to-group transfers are negative at some angles due to the truncation of the Legendre expansion, negative estimates may be obtained, and thus the total estimated fluence is reduced. The magnitude of the negative values is usually small compared to the positive values. This problem of negative contributions is not as great with the estimator S. This latter estimator chooses one outgoing group from the array and then performs the estimation only for that group. Thus, the more probable groups are chosen most often and have positive estimates. Few estimates are made with negative contributions.

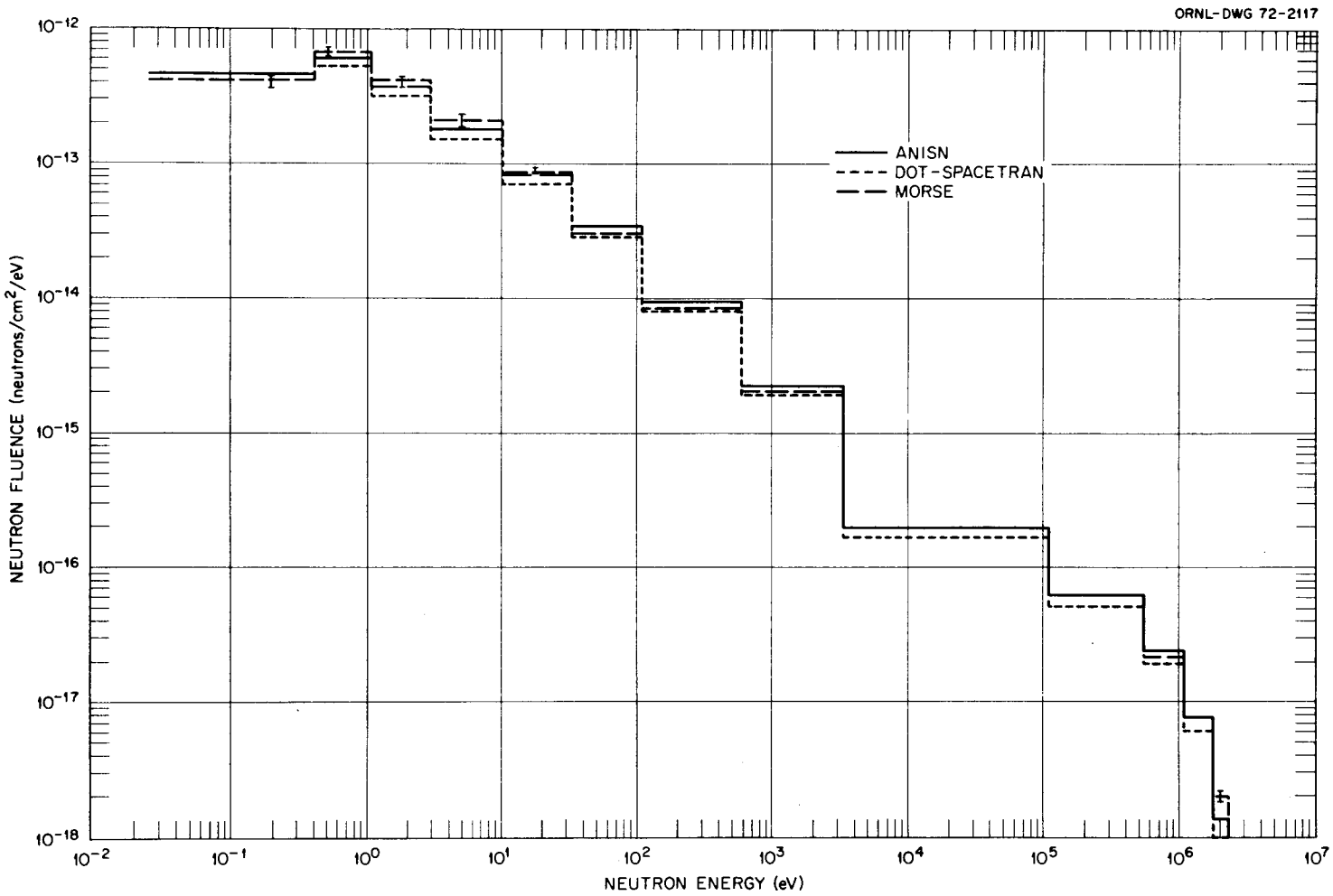

Neutron Energy Spectrum for 2.54 cm Slab, Detector 4.

Figure 3

Table 8 presents a condensation of the data in Tables 6 and 7. Given for each slab thickness and each detector is the fractional difference between DOT and ANISN results, MORSE and ANISN results, and 06R-OGRE and ANISN results. Thus, for detector number 4 for the 2.54-cm case, DOT (2) was low by 16% compared with ANISN, and MORSE was high by 5%. Also, this MORSE result had a 2% estimated fractional standard deviation. The MORSE results are the average of results obtained with each estimator, except for the neutron fluence for the 2.54-cm slab for detector 4 where only estimator S results are shown.

The results appear to agree very well with the following exceptions: DOT appears to be low for detectors 3 and 4 for the neutron fluence for both thicknesses and for gamma fluence for the 15.24-cm case. This is attributed to the quadrature set and the method currently used by SPACETRAN in interpolating between angles. The 100-angle asymmetric quadrature set used in these calculations has 16 polar angles exiting the slab toward the detectors. However, only 4 of these polar angles are between 45° and 90°, the rest being between 0° and 45°. For each mesh point on the end of the cylinder, SPACETRAN utilizes the angular leakage at the closest discrete angle. For each of the last two detectors, the closest direction is at a more oblique angle. Due to the rapid fall off in angular-dependent leakage with increasing angle, the SPACETRAN calculation will be low. This effect is seen in all but the 2.54-cm case gamma-ray fluence. In this latter case, the angular leakage does not fall off as rapidly as can be seen in Tables 6 and 7. Another possible cause for the progressively lower DOT results as the angle increases may be the side leakage from the DOT r-z geometry. For the 2.54-cm case, this side leakage is insignificant.

Table 8. Fractional Difference of DOT, MORSE, and 06R-OGRE Results Compared With ANISN Results

Detector Number	1	2	3	4
COSINE	0.98561	0.89632	0.73218	0.1447
		2.54-cm		
		Neutrons		
DOT(2)-ANISN	0.00	-0.04	-0.12	-0.16
MORSE-ANISN	+0.01(.01)	-0.01(.01)	-0.01(.01)	+0.05(.02)
06R-ANISN	-0.02(.01)	-0.01(.01)	+0.01(.01)	-0.07(.03)
		Gamma Rays		
DOT(2)-ANISN	-0.02	+0.01	+0.03	+0.07
MORSE-ANISN	-0.05(.04)*	-0.04(.04)	-0.05(.04)	-0.06(.04)
06R-OGRE-ANISN	-0.02(.04)	-0.02(.04)	-0.04(.04)	-0.06(.05)
		15.24-cm		
		Neutrons		
DOT-ANISN	-0.01	-0.06	-0.26	-0.19
MORSE-ANISN	+0.03(.03)	+0.05(.03)	-0.12(.04)	-0.11(.10)
06R-ANISN	+0.01(.04)	-0.02(.05)	-0.17(.07)	-0.24(.21)
		Gamma Rays		
DOT-ANISN	-0.04	-0.04	-0.09	-0.25
MORSE-ANISN	-0.02(.03)	-0.02(.03)	-0.02(.03)	+0.02(.04)
06R-OGRE-ANISN	+0.05(.04)	+0.05(.04)	+0.04(.04)	+0.05(.10)

*This entry indicates that MORSE yielded an answer 5% lower than ANISN for the total gamma-ray fluence for the 2.54-cm slab detector 1, and the MORSE results had a fractional standard deviation of 4%.

The side leakage is greater for the 15.24-cm case, particularly for gamma rays. For a more exact solution, the radius should be larger for the 15.24-cm case.

Another point of disagreement is the MORSE and 06R neutron results for detectors 3 and 4 for the 15.24-cm slab. This is attributed to underestimation by the next-flight estimators. The polar angles for the latter two detectors make this case a deep-penetration problem. In fact, if a collision occurs 2 cm from the side of the slab toward the detector, the actual thickness of polyethylene between the collision site and detector 4 is 13.8 cm. Thus, for the next-flight estimator to yield a meaningful estimate, a significant number of samples must be made of events near the surface of the slab. Other than non-leakage in the MORSE calculations, no attempt was made in importance sampling the collision sites near the surface of the slab to improve the results for this case.

The overall agreement between the results presented here is indeed satisfying. This agreement provides a degree of confidence in both the transport codes and cross-section processing codes, and also has been quite instructive for the author.

Acknowledgments

The author wishes to express his appreciation to G. W. Morrison for running the 06R and OGRE calculations, to L. R. Williams for preparing the multigroup cross sections, and to C. E. Clifford for his support and guidance throughout this work.

REFERENCES

1. E. A. Straker, P. N. Stevens, D. C. Irving, and V. R. Cain, "The MORSE Code - A Multigroup Neutron and Gamma-Ray Monte Carlo Transport Code," ORNL-4585 (1970).

2. F. R. Mynatt, F. J. Muckenthaler, and P. N. Stevens, "Development of Two-Dimensional Discrete Ordinates Transport Theory for Radiation Shielding," CTC-INF-952 (1969).

3. S. N. Cramer and M. Solomito, "SPACETRAN: A Code to Calculate Dose at Detectors at Various DistancesF scsceFrom the Surface of a Cylinder," ORNL-TM-2592 (1969).

4. W. W. Engle, Jr., "A User's Manual for ANISN," K-1693 (1967).

5. C. L. Thompson and E. A. Straker, "06R-ACTIFK, Monte Carlo Neutron Transport Code," ORNL CF 69-8-36 (1969).

6. D. K. Trubey and M. B. Emmett, "OGRE-G, An OGRE System Monte Carlo Code for the Calculation of Gamma-Ray Dose Rate at Arbitrary Points in an Arbitrary Geometry," ORNL-TM-1212 (1966).

7. V. R. Cain, "SAMBO, A Collision Analysis Package for Monte Carlo Codes," ORNL CF 70-9-1 (1970).

8. R. Q. Wright, J. L. Lucius, N. M. Greene, and C. W. Craven, Jr., "SUPERTOG: A Program to Generate Fine Group Constants and P_n Scattering Matrices From ENDF/B," ORNL-TM-2679 (1969).

9. J. R. Knight and F. R. Mynatt, "MUG, A Program for Generating Multigroup Photon Cross Sections," CTC 1-17 (1970).

10. W. E. Ford, III, and D. H. Wallace, "POPOP4, A Code For Converting Gamma-Ray Spectra to Secondary Gamma-Ray Production Cross Sections," CTC-12 (1969).

11. W. E. Ford, III, and J. S. Gillen, "The Testing of ^{238}U Secondary Gamma-Ray Production Data Sets From the POPOP4 Library," ORNL-TM-3482 (1971), Appendix B, page 105.

INTERNAL DISTRIBUTION

1-3. L. S. Abbott
4. R. G. Alsmiller, Jr.
5. T. W. Armstrong
6. A. R. Buhl
7. V. R. Cain
8-12. C. E. Clifford
13. S. N. Cramer
14. W. K. Crowley
15. M. B. Emmett
16. W. W. Engle, Jr.
17. W. E. Ford, III
18. R. M. Freestone, Jr.
19. T. A. Gabriel
20. N. M. Greene
21. M. L. Gritzner
22. T. J. Hoffman
23. J. L. Lucius
24. R. E. Maerker
25. F. C. Maienschein
26. B. F. Maskewitz
27. B. J. McGregor
28. G. W. Morrison
29. F. R. Mynatt
30. E. M. Oblow
31. R. W. Peelle
32. F. G. Perey
33. J. C. Robinson
34. R. W. Robinson
35. D. Sundberg
36. D. K. Trubey
37. G. E. Whitesides
38. L. R. Williams
39. H. A. Wright
40. R. Q. Wright
41. W. Zobel
42. H. Feshbach (consultant)
43. H. Goldstein (consultant)
44. C. R. Mehl (consultant)
45. H. T. Motz (consultant)
46-47. Central Research Library
48. ORNL Y-12 Technical Library Document Reference Section
49-51. Laboratory Records
52. Laboratory Records ORNL RC
53. ORNL Patent Office

EXTERNAL DISTRIBUTION

54. W. H. Hannum, Division of Reactor Development and Technology, U. S. Atomic Energy Commission, Washington, D. C. 20545
55. P. B. Hemmig, Division of Reactor Development and Technology, U. S. Atomic Energy Commission, Washington, D. C. 20545
56. K. O. Laughon, AEC Site Representative
57-150. Given Defense Nuclear Agency Shielding Distribution dated March 8, 1972.
151-170. C. E. Burgart, Science Applications, Inc., 122 LaBeta Dr., NE, Albuquerque, N. Mexico 87108
171. Laboratory and University Division, ORO
172. Division of Technical Information Extension, DTIE